

Direct lattice calculation of inclusive hadronic tau decay rates

A. Evangelista, R. Frezzotti¹, G. Gagliardi³, V. Lubicz^{2,3}, F. Sanfilippo³, S. Simula³, N. Tantalo¹

¹University and INFN of Rome Tor Vergata, ²University of Roma Tre, ³INFN, Section of Roma Tre

1 | Motivation

Inclusive hadronic τ decays are particularly interesting from the phenomenological viewpoint since they give access to V_{ud} and V_{us} . To date, the determinations of V_{us} from leptonic and semileptonic kaon decays and the ones obtained from inclusive hadronic τ decays present a tension [1]. On the lattice, hadronic τ decays have been studied by using dispersion relations and by combining non-perturbative lattice inputs with perturbative and/or OPE calculations (see for example [2]). Here we present a method to perform a fully non-perturbative lattice calculation of the $\tau \mapsto X \nu_\tau$ decay rate.

2 | Physical quantity and Lattice Approach

Assuming the Fermi point-like approximation for the weak interactions and neglecting radiative corrections, the inclusive hadronic decay rate $\Gamma[\tau \mapsto X_{fg} \nu_\tau]$, where f and g label the flavour quantum numbers of the final hadronic states, normalized with the rate $\Gamma[\tau \mapsto e \bar{\nu}_e \nu_\tau]$, can be expressed as

$$R_{fg} = 12\pi |V_{fg}|^2 \int_{r_{fg}}^1 d\omega \omega (1 - \omega^2)^2 \{F_L(\omega^2) + F_T(\omega^2) (1 + 2\omega^2)\}.$$

Here $\omega^2 = p_X^2/m_\tau^2$, with p_X the four-momentum of the hadronic state and $r_{fg} = m_{fg}/m_\tau$ is the ratio of the mass of the lightest hadronic state and the τ mass, while F_L and F_T are the longitudinal and transverse form factors parametrizing the hadronic spectral density

$$\mathcal{H}^{\mu\nu}(p_X) = p_X^\mu p_X^\nu F_L(\omega^2) + [p_X^\mu p_X^\nu - g^{\mu\nu} p_X^2] F_T(\omega)$$

that enters in the decay rate formula. In the reference frame where the final hadronic state is at rest, $p_X = (m_\tau \omega, \vec{0})$, we have

$$R_{fg} = 12\pi |V_{fg}|^2 \lim_{\sigma \rightarrow 0} \int_{r_{fg}}^\infty d\omega \{ \mathcal{H}^{ii}(\omega) K_\sigma^T(\omega) + \mathcal{H}^{00}(\omega) K_\sigma^L(\omega) \}$$

where we have introduced the smeared kernels

$$K_\sigma^L(\omega) = \frac{(1 - \omega^2)^2}{\omega} \Theta_\sigma(1 - \omega), \quad K_\sigma^T(\omega) = \frac{(1 - \omega^2)^2 (1 + 2\omega^2)}{3\omega} \Theta_\sigma(1 - \omega)$$

and a regularization of the step-function such that $\lim_{\sigma \rightarrow 0} \Theta_\sigma(\omega) = \theta(\omega)$. We considered

$$\Theta_\sigma^{(1)}(\omega) = \frac{1}{1 + e^{-\omega/\sigma}}, \quad \Theta_\sigma^{(2)}(\omega) = \frac{1}{1 + e^{-\sinh(\omega/\sigma)}}, \quad \Theta_\sigma^{(3)}(\omega) = \frac{1 + \text{Erf}(\omega/\sigma)}{2}.$$

Under the assumption that $\mathcal{H}^{\mu\nu}(\omega)$ is regular at $\omega = 1$, an analytical calculation shows that the corrections to the $\sigma \mapsto 0$ limit are even functions of σ , starting at $\mathcal{O}(\sigma^4)$, i.e.

$$\int_{r_{fg}}^\infty d\omega \mathcal{H}^{ii}(\omega) \{K_\sigma^T(\omega) - K_0^T(\omega)\} = \mathcal{O}(\sigma^4),$$

and similarly for the longitudinal case. The previous representation of R_{fg} allows a straightforward application of the algorithm of ref. [3] along the lines of refs. [4]. Indeed, by considering the euclidean correlator of the relevant weak currents,

$$C^{\mu\nu}(t) = \int d^3x \mathbb{T} \langle 0 | J_{fg}^\mu(t, \vec{x}) J_{fg}^{\nu\dagger}(0) | 0 \rangle, \quad J_{fg}^\mu = V_{fg}^\mu - A_{fg}^\mu,$$

the method of ref. [3] provides the coefficients $g^{L,T}(t, \sigma)$ such that

$$-\frac{2\pi}{m_\tau} \sum_{t=1}^{t_{\max}} g^L(t, \sigma) C^{00}(t) = \int_{r_{fg}}^\infty d\omega \mathcal{H}^{00}(\omega) K_\sigma^L(\omega)$$

and

$$\frac{2\pi}{m_\tau} \sum_{t=1}^{t_{\max}} g^T(t, \sigma) C^{ii}(t) = \int_{r_{fg}}^\infty d\omega \mathcal{H}^{ii}(\omega) K_\sigma^T(\omega)$$

within controllable statistical and systematic errors.

3 | The HLT method

In the algorithm of ref. [3] the $g^{L,T}$ coefficients are calculated by minimizing a linear combination of the norm functional, measuring the distance between the target and reconstructed kernel, and the error functional that regularizes the problem. Here we consider the norm functional

$$A_\alpha[g] = \int_0^\infty d\omega e^{\alpha m_\tau \omega} \left| \sum_{t=1}^{t_{\max}} g^{L,T}(t, \sigma) e^{-m_\tau \omega t} - K_\sigma^{L,T}(\omega) \right|^2$$

depending upon the real parameter $\alpha < 2$. By changing the relative weight between the norm and error functionals one can balance statistical and systematic errors. The latter are due to an imperfect reconstruction of the target smeared kernels, e.g.

$$\delta_{sys}^T = \left| \int_{r_{fg}}^\infty d\omega \mathcal{H}^{ii}(\omega) \left\{ \sum_{t=1}^{t_{\max}} g^T(t, \sigma) e^{-m_\tau \omega t} - K_\sigma^T(\omega) \right\} \right|.$$

For $\alpha > 0$ the difference between the target and the reconstructed kernel is forced to vanish exponentially at large energies where, conversely, hadronic spectral densities have a power-law growth. Therefore, the contribution to the systematic error coming from the high energy region is highly suppressed in the case $\alpha > 0$ with respect to the standard choice $\alpha = 0$. As in ref. [5], we check the onset of the statistical dominated regime by comparing the results obtained with two different norm functionals, which in our case corre-

spond to A_α for $\alpha = 2^-$, $\alpha = 1$ and $\alpha = 0$.

4 | Results

The numerical results presented here have been obtained by using the light-quarks ($f = u, g = d$) vector-vector ($C_V^{\mu\nu}$) and axial-axial ($C_A^{\mu\nu}$) renormalized correlators [6] produced by the ETM Collaboration on the ensemble cB211.072.64 with physical pion mass, $a = 0.08$ fm and $L = 5.12$ fm [7]. In each channel we considered both Osterwalder-Seiler (OS) and Twisted-Mass (TM) valence quarks corresponding to two discretizations, differing for $\mathcal{O}(a^2)$ terms, of the same continuum correlator. In the following figures, we show the calculation of the transverse contribution to R_{ud} coming from the C_A^{ii} correlator.

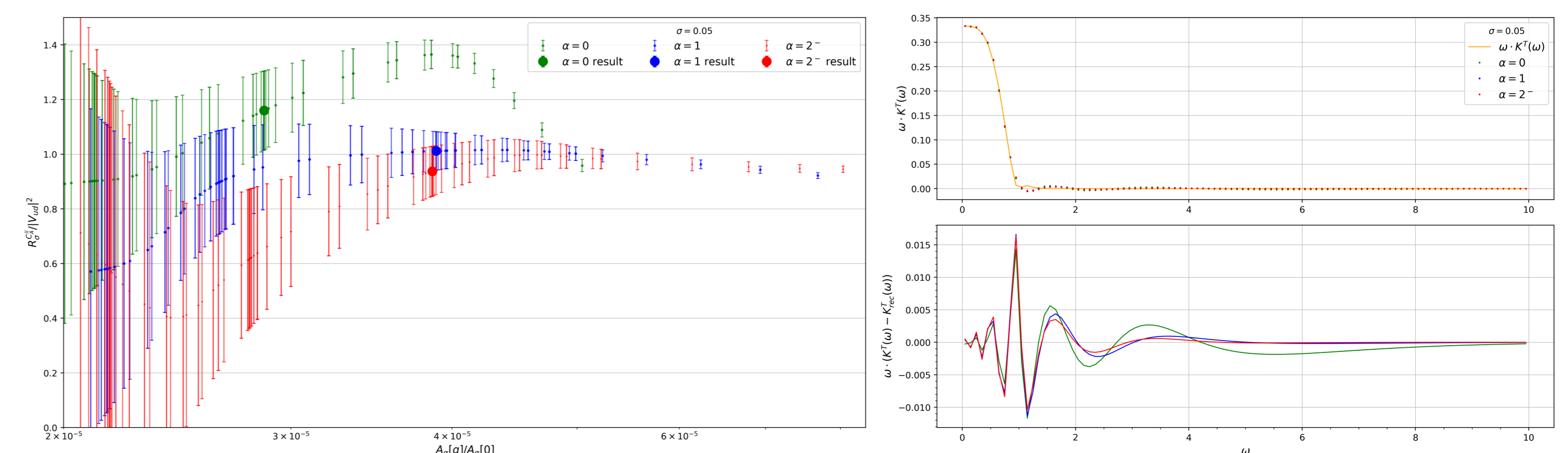


Figure 1: Left: the contribution to $R_{ud}/|V_{ud}|^2$, obtained from the HLT algorithm with $\alpha = 0$ (green), $\alpha = 1$ (blue) and $\alpha = 2^-$ (red), is plotted against $A_{\alpha=0}[g]/A_{\alpha=0}[0]$. The red, blue and green points and error bars show our best estimates for the three cases. Right: the reconstructed kernel $K^T(\omega)$ corresponding to the red, blue and green points and their differences with respect to the target kernel (solid orange curve) are shown.

From the $\alpha = 1$ data, that are particularly stable and fully consistent with the $\alpha = 2^-$ ones (see Fig. 1), we extract our final result. For the two different lattice discretizations we perform two separate combined fits to the data from the three kernels with ansatz $f_{fit} = c_0 + c_{1,k} \cdot \sigma^4 + c_{2,k} \cdot \sigma^6$, where $k = 1, 2, 3$ labels the smearing kernel type. The difference in the results gives a first rough estimate of the $\mathcal{O}(a^2)$ artifacts. In the following figure we show the individual contributions from the lattice correlators as well as the best fit plot in the case of the TM regularization.

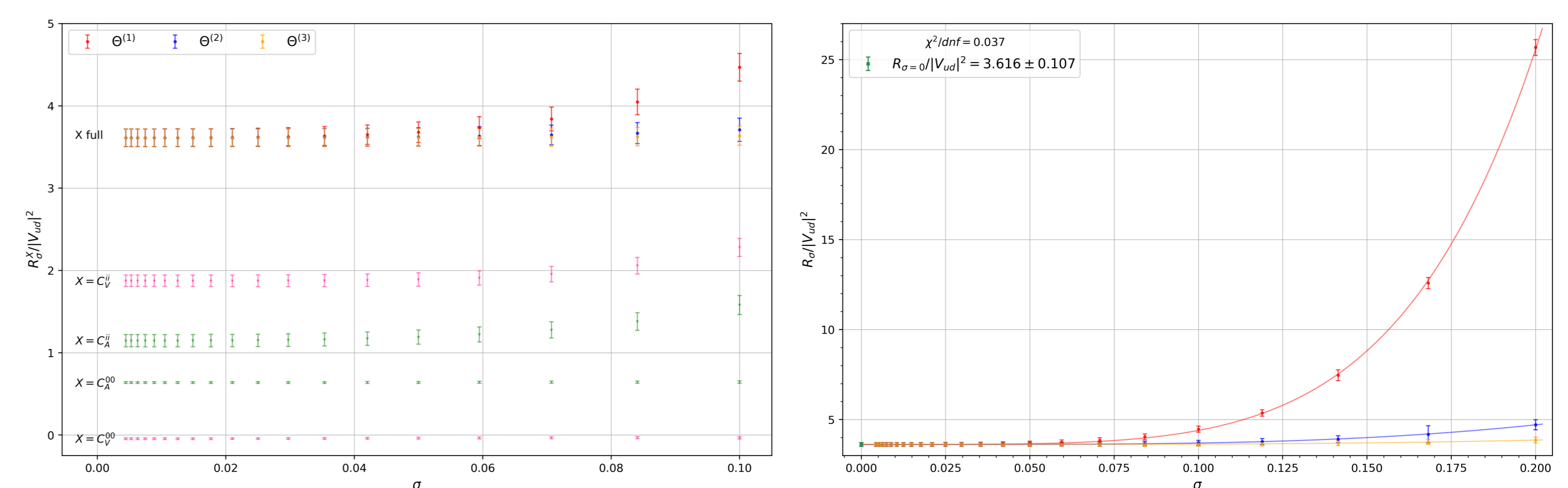


Figure 2: Left: the total decay rate $R_{ud}/|V_{ud}|^2$ obtained using $k = 1, 2, 3$ as a function of σ , as well as the contributions to it from C_V^{00} , C_V^{ii} , C_A^{ii} and C_A^{00} only for the case of $\Theta_\sigma^{(1)}$. Right: $R_{ud}/|V_{ud}|^2$ using $k = 1, 2, 3$ as a function of σ in a wider σ -range; furthermore, the best combined fit curves for each kernel (solid curves) and the extrapolated result at $\sigma = 0$ (point in dark-green) are shown.

5 | Outlook

Our preliminary one lattice spacing result for $R_{ud}/|V_{ud}|^2$ is the average of the estimates in the two discretizations: 3.533 ± 0.100 (OS) and 3.616 ± 0.107 (TM).

It differs from the HFLAV 2022 + Hardy and Towner result [8, 9] by 1.2 σ .

	HFLAV 2022 + Hardy and Towner	This work
$R/ V_{ud} ^2$	3.6615 ± 0.0078	3.572 ± 0.073

In order to control/remove lattice artifacts and possible finite size effects, a systematic study is planned using several lattice spacings and physical volumes. Moreover, we will extend this approach to lattice correlators with the weak up-strange currents in order to extract also $R_{us}/|V_{us}|^2$ and hence the V_{us} CKM matrix element. For high precision computations of the τ decay rates also the QED and strong isospin corrections should be evaluated.

References

- [1] Y. Aoki et al. “FLAG Review 2021”. In: (Nov. 2021). eprint: 2111.09849.
- [2] Peter Boyle et al. “Novel $|V_{us}|$ Determination Using Inclusive Strange τ Decay and Lattice Hadronic Vacuum Polarization Functions”. In: *Phys. Rev. Lett.* 121.20 (2018). eprint: 1803.07228.
- [3] Martin Hansen, Alessandro Lupo, and Nazario Tantalo. “Extraction of spectral densities from lattice correlators”. In: *Phys. Rev. D* 99 (9 May 2019), p. 094508.
- [4] Paolo Gambino et al. “Lattice QCD study of inclusive semileptonic decays of heavy mesons”. In: *JHEP* 07 (2022). eprint: 2203.11762.
- [5] John Bulava et al. “Inclusive rates from smeared spectral densities in the two-dimensional $O(3)$ non-linear σ -model”. In: (Nov. 2021). eprint: 2111.12774.
- [6] C. Alexandrou et al. “Lattice calculation of the short and intermediate time-distance hadronic vacuum polarization contributions to the muon magnetic moment using twisted-mass fermions”. In: (June 2022). eprint: 2206.15084.
- [7] Constantia Alexandrou et al. “Simulating twisted mass fermions at physical light, strange and charm quark masses”. In: *Phys. Rev. D* 98.5 (2018). eprint: 1807.00495.
- [8] Y. Amhis et al. “Averages of b -hadron, c -hadron, and τ -lepton properties as of 2021”. In: (June 2022). eprint: 2206.07501.
- [9] J. C. Hardy and I. S. Towner. “Superallowed $0^+ \rightarrow 0^+$ nuclear β decays: 2020 critical survey, with implications for V_{ud} and CKM unitarity”. In: *Phys. Rev. C* 102 (4 Oct. 2020), p. 045501.